

BioCell Your Trusted Supplier of *in vivo* MAbs
α-PD-1 · α-PD-L1 · α-CTLA-4 · α-CD20 · α-NK1.1 · α-IFNAR-1

DISCOVER MORE



A Poxvirus Protein That Binds to and Inactivates IL-18, and Inhibits NK Cell Response

This information is current as of August 4, 2022.

Teresa L. Born, Lynda A. Morrison, David J. Esteban, Tim VandenBos, Lydia G. Thebeau, Nanhai Chen, Melanie K. Spriggs, John E. Sims and R. Mark L. Buller

J Immunol 2000; 164:3246-3254; ;
doi: 10.4049/jimmunol.164.6.3246
<http://www.jimmunol.org/content/164/6/3246>

References This article **cites 53 articles**, 23 of which you can access for free at:
<http://www.jimmunol.org/content/164/6/3246.full#ref-list-1>

Why *The JI*? [Submit online.](#)

- **Rapid Reviews! 30 days*** from submission to initial decision
- **No Triage!** Every submission reviewed by practicing scientists
- **Fast Publication!** 4 weeks from acceptance to publication

*average

Subscription Information about subscribing to *The Journal of Immunology* is online at:
<http://jimmunol.org/subscription>

Permissions Submit copyright permission requests at:
<http://www.aai.org/About/Publications/JI/copyright.html>

Email Alerts Receive free email-alerts when new articles cite this article. Sign up at:
<http://jimmunol.org/alerts>



A Poxvirus Protein That Binds to and Inactivates IL-18, and Inhibits NK Cell Response¹

Teresa L. Born,* Lynda A. Morrison,[†] David J. Esteban,[†] Tim VandenBos,* Lydia G. Thebeau,[†] Nanhai Chen,[†] Melanie K. Spriggs,* John E. Sims,*² and R. Mark L. Buller^{†3}

IL-18 induces IFN- γ and NK cell cytotoxicity, making it a logical target for viral antagonism of host defense. We demonstrate that the ectromelia poxvirus p13 protein, bearing homology to the mammalian IL-18 binding protein, binds IL-18, and inhibits its activity in vitro. Binding of IL-18 to the viral p13 protein was compared with binding to the cellular IL-18R. The dissociation constant of p13 for murine IL-18 is 5 nM, compared with 0.2 nM for the cellular receptor heterodimer. Mice infected with a p13 deletion mutant of ectromelia virus had elevated cytotoxicity for YAC-1 tumor cell targets compared with control animals. Additionally, the p13 deletion mutant virus exhibited decreased levels of infectivity. Our data suggest that inactivation of IL-18, and subsequent impairment of NK cell cytotoxicity, may be one mechanism by which ectromelia evades the host immune response. *The Journal of Immunology*, 2000, 164: 3246–3254.

Interleukin-18, a recently characterized cytokine produced by activated macrophages, stimulates IFN- γ production, induces NK cell cytotoxicity, and participates in the polarization of the T-lymphocyte Th1 phenotype (1, 2). IL-18 was originally identified as IFN- γ inducing factor, purified from the livers of mice following induction of toxic shock (3). LPS-induced liver damage is in fact prevented upon inhibition of IL-18 by neutralizing Abs (3) or in IL-18-deficient mice (4). IL-18 has been shown to increase IFN- γ production in Ag-stimulated T cell lines, and to act synergistically with IL-12 to stimulate IFN- γ production in Th1 clones (5, 6). In NK cells, IL-18 enhances IFN- γ production (7, 8) and stimulates cytotoxicity (3). IL-18-deficient mice display reduced NK cell killing activity (4) and treatment of wild-type (WT)⁴ mice with exogenous IL-18 augments NK cell cytotoxicity in vitro and in vivo (4, 9, 10).

IL-18 is structurally related to the IL-1 family of cytokines (11) and has been shown to be processed by the IL-1 β -converting enzyme (12, 13). Furthermore, the IL-18R is related to the IL-1 family of receptors, being composed of a ligand-binding subunit, IL-1Rrp1 (14, 15) and an accessory subunit, AcPL (16), both of which share sequence homology to the IL-1R family. It has been proposed that synergy observed between IL-12 and IL-18 may be due to the induction of IL-18R expression by IL-12 in B and T cells (17, 18).

A soluble protein has recently been described which binds and inhibits IL-18, yet bears no significant homology to either IL-18R subunit (19). The IL-18 binding protein (IL-18BP) contains a single putative Ig domain. This Ig domain bears very limited homology to the third Ig domain of the type II IL-1R. Much greater homology to IL-18BP can be found in a family of proteins (p13/p16) encoded by several poxviruses (swinepox, cowpox, variola, molluscum contagiosum, and ectromelia) (19, 20).

Poxviruses infect the host mainly through the cornified epithelium of the skin or the mucosal surface of the respiratory tract. The skin probably becomes infected through microscopic abrasions, which allows the virus access to the epidermal and dermal layers. In these layers the poxvirus replicates locally, and most species of virus rapidly spread to the draining lymph node via the lymphatics, and possibly also via infected cells (21). Some poxviruses, such as molluscum contagiosum, cause a localized, self-limited infection. Others cause a fulminant, systemic infection characterized by a generalized rash and high mortality rate, as with variola virus (smallpox), human monkeypox, or ectromelia virus (EV) (mousepox). In either case, virus transmission usually originates from infection in the epithelia and persists in the face of circulating systemic immunity (21).

Poxviruses often acquire cellular proteins critical for immune regulation, thus allowing them to escape host responses (22). The first such protein identified was encoded by the T2 open reading frame (ORF) of Shope fibroma poxvirus. This ORF produced a secreted soluble form of the type II TNF receptor (23) which, when deleted in myxoma poxvirus, reduced virulence by nearly 70% (24). Indeed, many of the viral immune regulators subsequently identified represent soluble versions of cellular cytokine receptors (i.e., type II IL-1, type II TNF, and type I and type II IFN receptors), although some, such as the secreted p35 protein from variola and cowpox viruses, bind and neutralize their target molecules (β -chemokines) despite being structurally unrelated to the cellular receptor (25–28).

We have examined the capacity of the EV homologue within the p13/p16 family (subsequently referred to as p13) to bind IL-18 and inhibit its function both in vitro and in vivo. We show that p13 binds IL-18 with nanomolar avidity, that p13 inhibits the binding of IL-18 to its cellular receptor, and that it inhibits the biological activity of IL-18 in vitro. Intraperitoneal infection of mice with a

*Immunex Corporation, Seattle WA 98101; and [†]Department of Molecular Microbiology and Immunology, Saint Louis University, St. Louis, MO 63104

Received for publication August 23, 1999. Accepted for publication January 5, 2000.

The costs of publication of this article were defrayed in part by the payment of page charges. This article must therefore be hereby marked *advertisement* in accordance with 18 U.S.C. Section 1734 solely to indicate this fact.

¹ Support for the portion of these studies conducted at Saint Louis University was provided by the Elsa U. Pardee Foundation (to R.M.L.B.)

² Address correspondence and reprint requests to Dr. John E. Sims, Department of Molecular Biology, Immunex Corporation, 51 University Street, Seattle, WA 98101. E-mail address: jsims@immunex.com

³ Address correspondence and reprint requests to Dr. R. Mark L. Buller, Department of Molecular Microbiology and Immunology, 1402 South Grand Boulevard, Saint Louis University, St. Louis, MO 63104. E-mail address: bullerm@slu.edu

⁴ Abbreviations used in this paper: WT, wild type; AcPL, accessory protein-like; IL-18BP, IL-18 binding protein; ORF, open reading frame; EV, ectromelia virus; m, murine; s, soluble; RRU, relative response units; PEC, peritoneal exudate cell; p.i., postinfection.

WT vs a p13 knockout form of EV indicates that p13 down-regulates NK cell cytotoxic activation in vivo. Furthermore, deletion of p13 results in decreased viral infectivity in the liver.

Materials and Methods

Plasmid construction and protein purification

EV p13 ORF has been described (20). It was amplified by PCR and subcloned into pDC409 (29) as a fusion with the CH2 and CH3 domains of human IgG1 (30). Expression vectors encoding murine (m)IL-1Rrp1, mAcPL, soluble (s)IL-1Rrp1-Fc, and sAcPL-Fc have been described previously (16). Plasmids encoding fusions with FlagpolyHis contain the same gene-specific regions as the above described plasmids, but the mutein Fc has been replaced with the peptide RSDYKDDDDKPGHHHHHHHPG. The luciferase reporter plasmid containing three multimerized NF- κ B sites and a minimal c-Fos promoter has been described previously (31). The murine IL-18 sequence was cloned into pDC206 (3, 32).

Following transient transfection of CV-1/EBNA cells by the DEAE-dextran method (33), fusion proteins were purified from culture supernatants by chromatography on protein A-Poros or Nickel columns (PerSeptive Biosystems, Framingham, MA). Purity and relative amounts of each Fc protein were assessed by PAGE, and purity was consistently found to be >98%. Furthermore, the N-terminal sequence was determined after each independent purification, to verify the identity of the purified protein. Mixed heterodimeric proteins yielded sIL-1Rrp1 sequence, presumably due to the observation that sAcPL-Fc was expressed at significantly lower levels than sIL-1Rrp1-Fc. Protein was quantitated by amino acid analysis and by the BCA method (Pierce, Rockford, IL).

Cell culture and transfection

COS-7 and BS-C-1 cells were maintained in DMEM/5% and 10% FBS, respectively. To assess inhibition of NF- κ B activation, COS-7 cells were transiently transfected by the DEAE for consistency dextran method with 10 ng of each receptor plasmid (mIL-1Rrp1 and mAcPL) and 50 ng of the reporter plasmid per 4.5×10^4 cells. The total amount of DNA in the transfection was increased to 1 μ g/well by addition of empty pDC304 vector. Two days posttransfection, mIL-18 (PeproTech, Rocky Hill, NJ) (20 ng/ml final concentration) was preincubated with varying amounts of Fc fusion protein (3–12 μ g/ml final concentration) for 15 min at room temperature. Transfected cells were stimulated with the pretreated mIL-18 for 4 h, at which time cells were lysed and luciferase activity assessed using Reporter Lysis Buffer and Luciferase Assay Reagent (Promega, Madison, WI).

Immunoprecipitation of [35 S]IL-18

COS-7 cells (4.5×10^4) were transiently transfected by the DEAE-dextran method with an empty expression plasmid, or the same plasmid encoding mIL-18 (1 μ g each). Two days posttransfection, cells were starved for 1 h then labeled in [35 S]Cys-[35 S]Met containing medium for 4 h. The supernatants were removed, subjected to centrifugation, and adjusted to 0.4 M NaCl/1.0% Triton X-100 in the presence of protease inhibitors. Fc fusion protein (1 μ g) was added to the supernatants along with 30 μ l of a 50% slurry of protein G-Sepharose (Boehringer Mannheim, Indianapolis, IN). As indicated, various amounts of FlagpolyHis fusion proteins were also included in the immunoprecipitations. Following precipitation overnight at 4°C, immunocomplexes were washed extensively in buffer (0.4 M NaCl, 0.05% SDS, and 1.0% Nonidet P-40) and then separated by electrophoresis in a 4–20% Tris-Glycine gel (Novex, San Diego, CA). The gel was fixed, incubated in Amplify (Amersham Pharmacia Biotech, Piscataway, NJ), dried, and exposed to X-OMAT AR film (Eastman Kodak, Rochester, NY).

BIAcore binding

Binding of mIL-18 to the Fc fusion proteins was evaluated using the BIAcore 3000 (Pharmacia Biacore, Uppsala, Sweden). All binding experiments were performed at 25°C. Goat anti-human IgG (Jackson ImmunoResearch, West Grove, PA) was immobilized to a CM5 BIAcore sensor chip via amine coupling at pH 4.8 as previously described (34). The Fc proteins were then loaded onto the surface at equimolar levels of protein. Various levels of mIL-18 (0.15 nM to 1 μ M) in 3-fold serial dilutions were then run over the flow cells for 6 min at 10 μ l/min and then allowed to dissociate for 20 min. Between binding cycles the flow cell was regenerated using 100 mM glycine (pH 1.65) plus 0.15 M NaCl, then reloaded with Fc protein before addition of the next higher concentration of mIL-18. Before evaluation, a background curve of the same concentration of mIL-18 run over a surface coated with capture Ab only was subtracted. Data was evaluated using the BIAcore BIA Evaluation 3.0.2 software

(Pharmacia Biacore). All data obtained were utilized in the data evaluation except in the case of p13-Fc, where we only used the data from 0.15 to 111 nM to determine the binding constant.

Construction of EV-p13 $^{-}$

The p13 gene in pL28-5 (20) was inactivated by the insertion of a 2-kbp cassette containing the *Escherichia coli* guanine phosphoribosyltransferase (gpt) gene under the control of the vaccinia virus 7.5 K promoter (20). The mutated gene was transfected into CV-1 cells coinfecting with WT EV, and a recombinant mutant virus (EV-gpt $^{+}$, p13 $^{-}$; hereafter EV-p13 $^{-}$) was selected by three plaque purifications in the presence of 25 μ g/ml of mycophenolic acid, 250 μ g/ml xanthine, and 15 μ g/ml hypoxanthine. The genotype of EV-p13 $^{-}$ was verified by PCR using combinations of primers 5' and 3' to the p13 gene and the selection cassette. The mutant virus was expanded in BS-C-1 cells (35) and stored as a cell lysate at -70°C .

Animals

Specific-pathogen-free, female, C57BL/6 mice (Charles River Laboratories, Wilmington, MA) were procured through the National Cancer Institute (Frederick, MD) and used at 6–8 wk of age. Mice were treated in accordance with institutional policies and the Guide for Care and Use of Laboratory Animals.

Virus infection

Groups of mice were injected i.p. with 1×10^4 PFU of EV-WT, EV-p13 $^{-}$, or saline. At 1, 2, or 3 days postinfection (p.i.) mice were euthanized, the peritoneal cavities were washed with a total of 8 ml of HBSS, and the spleens and livers were removed. Peritoneal exudate cells (PECs) were pooled, washed, and enumerated. Splenocytes from two mice per group were pooled, and the mononuclear fraction was isolated using Lymphocyte Separation Medium (ICN Biomedicals, Costa Mesa, CA). Virus infectivity was determined as described previously (36).

Cytotoxicity assays

Standard ^{51}Cr -release assays to measure NK cytotoxic activity in splenocyte and PEC populations were performed as described in detail elsewhere (37), except that target cells were labeled for 2 h and 1×10^4 cells were added per well. In vitro depletion of CD8 $^{+}$ or NK cells from PECs before use in the ^{51}Cr -release assay was conducted by incubation for 30 min at 37°C with a mAb specific for CD8 (clone 2.43; rat IgG2b), or by sequential incubation of cells with anti-CD8 and anti-asialo-GM1 (Wako Pure Chemicals, Richmond, VA) and human complement (adsorbed on mouse splenocytes before use). An aliquot was analyzed by flow cytometry to assess efficacy of depletion. Cells were added to target without adjustment for reduction in cell number.

Flow cytometry

PECs were incubated with Fc block (PharMingen, San Diego, CA) for 15 min at 4°C, then aliquots were stained with FITC-conjugated anti-NK1.1 (clone PK136, mouse IgG2a; PharMingen), FITC-anti-CD4 (clone RM2501, rat IgG2a; Caltag Laboratories, Burlingame, CA), or FITC-anti-CD8 (clone CT-CD8a, rat IgG2a; Caltag Laboratories) at 0.5 μ g/10 6 cells in FACS buffer for 30 min at 4°C. A total of 7,000–10,000 cells were analyzed by flow cytometry using a FACSCalibur flow cytometer and CellQuest analysis software (Becton Dickinson, San Jose, CA).

Measurement of IFN- γ and IL-10 cytokines

Cultures of 1×10^6 splenocytes or PECs were incubated in 96-well plates for 5.5 h in RPMI plus 2% FCS with 50 μ g/ml PMA and 500 ng/ml calcium ionophore. Culture supernatants were harvested and frozen until cytokines were assayed. IFN- γ and IL-10 were detected by a sandwich ELISA protocol using an anti-IFN- γ mAb (clone 37801.11; R&D Systems, Minneapolis, MN) and an anti-IL-10 mAb (JES5-2A5; PharMingen) as capture reagents. Bound IFN- γ and IL-10 were detected by addition of biotinylated goat anti-mouse IFN- γ polyclonal Ab (R&D Systems) and biotinylated rat anti-mouse IL-10 mAb (SXC-1, PharMingen), respectively, followed by streptavidin-HRP (Zymed Laboratories, South San Francisco, CA) and the substrate *o*-Phenylenediamine. The optical density was measured at 490 nm and was converted to ng/ml using sets of IFN- γ and IL-10 standards. Each value is a geometric mean of cultures from three individual mice. Statistical significance was determined using the unpaired *t* test.

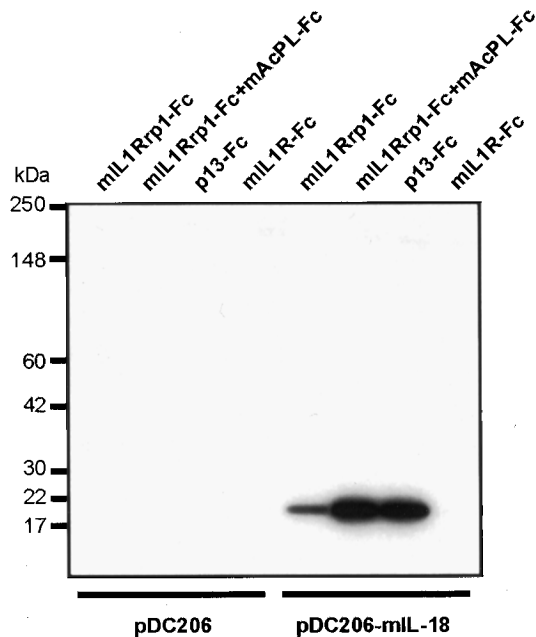


FIGURE 1. EV p13 binds mIL-18 *in vitro*. COS-7 cells were transfected with empty vector (pDC206) or the same vector encoding mIL-18 (pDC206-mIL-18), and 2 days posttransfection the samples were labeled with [³⁵S]Cys/Met-containing medium. The Fc fusion proteins (1 μg) indicated at the *top* of the figure, and protein G-Sepharose, were added to the labeled supernatants and precipitation was conducted overnight. The immunoprecipitated proteins were separated on 4–20% Tris-glycine gels, dried, and exposed to film. The autoradiogram following a 2-day exposure is shown.

Results

EV p13 binds IL-18 *in vitro*

The recently reported IL-18BP displays extremely limited similarity to the third putative Ig domain of the ligand binding subunit of the IL-18R, IL-1Rrp1 (19). IL-18BP shows higher homology to the EV p13 protein: 23.7% identity over 118 aa compared with 16.2% identity over 105 aa with IL-1Rrp1 (T. L. Born, unpublished observation). Therefore, we examined whether EV p13 was able to bind IL-18, and compared this binding with the binding of IL-18 to its cellular receptor.

It has been shown that the extracellular domain of IL-1Rrp1 (sIL-1Rrp1-Fc) is able to bind IL-18, whereas the extracellular region of the accessory subunit of the IL-18R (sAcPL-Fc) is unable to bind IL-18 under the same conditions (14–16). Dimerization of the extracellular regions of IL-1Rrp1 and AcPL, as demonstrated by co-expression of the soluble Fc fusion proteins in the same cell, creates a higher avidity IL-18R protein (T. L. Born and J. E. Sims, unpublished observation). Protein purified from the supernatant of cells co-transfected with sIL-1Rrp1-Fc and sAcPL-Fc contains, theoretically, 25% sIL-1Rrp1-Fc homodimers, 25% sAcPL-Fc homodimers, and 50% Fc heterodimers. To investigate the ability of IL-18 to bind these receptor proteins or the EV p13 protein, we incubated radiolabeled mIL-18 with equal amounts of sIL-1Rrp1-Fc, heterogeneous sIL-1Rrp1-Fc + sAcPL-Fc, or p13-Fc. Precipitation of the Fc proteins using protein G-Sepharose revealed that the mixed heterodimeric receptor and the p13 protein bound similar amounts of IL-18, whereas a lesser amount of IL-18 was bound by the IL-1Rrp1 homodimer (Fig. 1). We observed binding of p13-Fc to both murine and human IL-18, whereas receptor homodimers and heterodimers both failed to display cross-species binding (data not shown). The mammalian IL-18BPs are similarly able to bind either human or murine IL-18 (19). In sum-

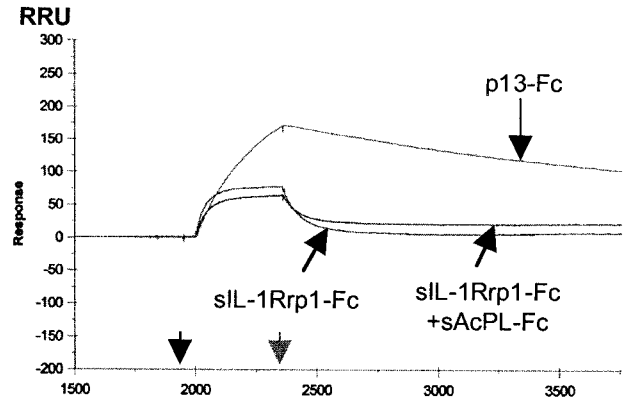


FIGURE 2. Binding of IL-18 to immobilized sIL-1Rrp1-Fc, sIL-1Rrp1-Fc + sAcPL-Fc, and p13-Fc. Individual BIAcore flow cells were loaded with either murine sIL-1Rrp1-Fc (20 μg/ml), murine sIL-1Rrp1-Fc + sAcPL-Fc (20 μg/ml), or EV p13-Fc (12 μg/ml). These amounts were calculated to be equimolar. The immobilized proteins were reacted with mIL-18 at the time indicated by the black arrow. After 6 min the IL-18 was removed (gray arrow). The background level of binding to capture Ab alone was subtracted from each sample.

mary, under the conditions tested, the avidity of IL-18 for p13 and for the receptor heterodimer appears to be higher than its avidity for IL-1Rrp1 alone. Specificity was demonstrated in that type I sIL-1R-Fc did not bind IL-18 under the same conditions (Fig. 1).

To investigate further the avidity of p13 for IL-18, we used BIAcore analysis to compare the binding of mIL-18 to sIL-1Rrp1-Fc, to the heterogeneous sIL-1Rrp1-Fc + sAcPL-Fc, and to p13-Fc. Flow cells were loaded with equimolar amounts of sIL-1Rrp1-Fc, sIL-1Rrp1-Fc + sAcPL-Fc mixed dimers, or p13-Fc and increasing concentrations of mIL-18 (0.15 nM to 1 μM) were exposed to the chip. Rapid binding of mIL-18 to sIL-1Rrp1-Fc was observed, which quickly returned to baseline following the removal of IL-18 (Fig. 2). Analysis of the data over the entire range of IL-18 concentrations tested demonstrates that sIL-1Rrp1-Fc binds to mIL-18 with a dissociation constant of 39 nM ($\chi^2 = 0.897$) (Table I). This avidity is in agreement with the affinity reported previously for both soluble and full-length IL-1Rrp1 (14, 15).

Binding of mIL-18 to the heterogeneous sIL-1Rrp1-Fc + sAcPL-Fc was of a similar magnitude but remained ~20% above baseline following removal of IL-18 (Fig. 2), suggesting a slower dissociation rate of the cytokine from the receptor heterodimer. This result is consistent with the immunoprecipitation results reported above. The data were fit with a heterogeneous ligand/parallel reaction model ($\chi^2 = 1.16$) because the Fc proteins represent a mixture of receptor heterodimers and homodimers. A portion of

Table I. BIAcore affinity measurements^a

Protein	k_a ($M^{-1} s^{-1}$)	k_d (s^{-1})	K_D (nM)
sIL-1Rrp1-Fc	2.68×10^5	1.05×10^{-2}	39
sIL-1Rrp1-Fc + sAcPL-Fc ^b	2.64×10^5	1.34×10^{-2}	51
sIL-1Rrp1-Fc + sAcPL-Fc ^c	4.80×10^5	1.04×10^{-4}	0.2
p13-Fc	0.79×10^5	4.55×10^{-4}	5

^a At least two individual experiments were conducted for each protein, using either 20 μg/ml of receptor Fc protein or 12 μg/ml of p13-Fc protein (equimolar amounts) to load the flow cell.

^b The near-identity of these values to those observed with sIL-1Rrp1-Fc allows us to assign this portion of the binding to IL-1Rrp1-Fc homodimers.

^c The significant difference of these values from those seen with sIL-1Rrp1-Fc lead us to assign this portion of the binding to sIL-1Rrp1-Fc/sAcPL-Fc heterodimers.

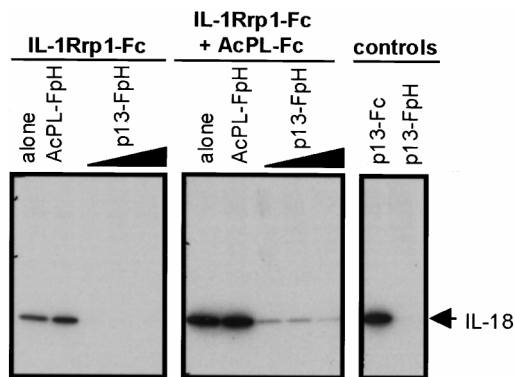


FIGURE 3. EV p13 inhibits binding of IL-18 to its receptor. Radiolabeled IL-18 was immunoprecipitated with 1 μ g of the Fc fusion protein indicated at the top of the figure, as described in Fig. 1. Additionally, 0.5, 2.0, or 5.0 μ g of FlagpolyHis fusion protein was added to the immunoprecipitations as a competitor. Labeled IL-18 was immunoprecipitated with either 1 μ g of p13-Fc (positive control) or 1 μ g of p13-FlagpolyHis (negative control) without competitor.

the binding was of an avidity similar to that observed for sIL-1Rrp1-Fc (51 nM), whereas the other binding component displayed a dissociation constant of 0.2 nM (Table I). We interpret this latter result to represent binding to receptor heterodimers in the heterogeneous preparation. Thus, heterodimerization of the receptor results in an \sim 100-fold increase in avidity for mIL-18.

The flow cell coated with p13-Fc generally displayed a greater overall RRU shift in response to IL-18 as compared with either of the receptor-Fc proteins. Moreover, both the association and dissociation of IL-18 from p13-Fc were much slower than was observed with the receptor homodimer or heterodimer (Fig. 2). Analysis of the data over the range of 0.15–111 nM mIL-18 indicates that p13-Fc has a dissociation constant of 5 nM ($\chi^2 = 1.73$) (Table I). This avidity is intermediate between the avidities of IL-18 for sIL-1Rrp1-Fc and for the putative heterodimeric portion of sIL-1Rrp1-Fc + sAcPL-Fc.

As a control, IL-1 β was run over flow cells coated with the same proteins and no shift was observed (data not shown). Taken together, these results suggest that mIL-18 has a higher avidity for the heterodimeric IL-1Rrp1 + AcPL than it does for IL-1Rrp1 or EV p13.

EV p13 inhibits the binding of IL-18 to its receptor

Although the mammalian IL-18BP was shown to inhibit the activity of IL-18 (19), it was never formally shown that binding of IL-18 to IL-18BP prevents binding to the cellular receptor. It is possible that p13 binds IL-18 at a site distinct from that of cellular receptor binding. To address this question, radiolabeled IL-18 was bound to sIL-1Rrp1-Fc or to sIL-1Rrp1-Fc + sAcPL-Fc in the presence of increasing amounts of p13-FlagpolyHis protein. The amount of 35 S-labeled IL-18 bound to the receptors was analyzed by precipitation with protein G-Sepharose. As shown in Fig. 3, an \sim 6-fold molar excess of sAcPL-FlagpolyHis had no effect on the binding of IL-18 to sIL-1Rrp1-Fc, whereas the same molar ratio of p13-FlagpolyHis completely ablated the observed binding. Similarly, addition of a 6-fold molar excess of sAcPL-FlagpolyHis had no effect on the binding of IL-18 to sIL-1Rrp1-Fc + sAcPL-Fc, yet 4-, 16-, and 38-fold excesses of p13-FlagpolyHis reduced, in a dose-dependent manner, the amount of IL-18 binding to the mixed heterodimeric receptor-Fc protein. We show in this experiment that p13-Fc efficiently bound and precipitated IL-18, whereas no IL-18 was precipitated with p13-FlagpolyHis, indicating that the

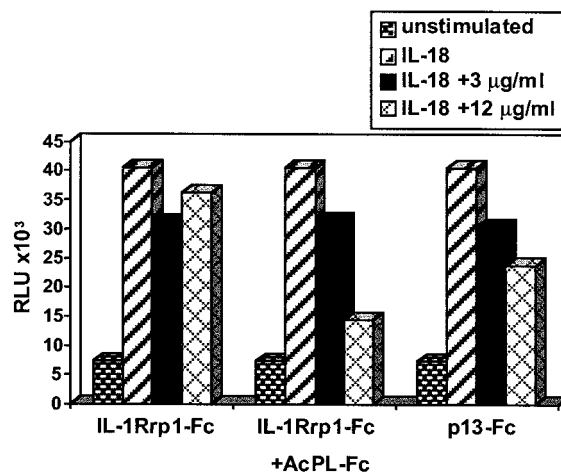


FIGURE 4. p13 inhibits the biological activity of IL-18. COS-7 cells were transiently transfected with 10 ng each of full-length mIL-1Rrp1 and mAcPL and 50 ng of 3 \times NF- κ B-luciferase reporter plasmid. Two days posttransfection cells were stimulated with PBS, 20 ng/ml mIL-18, or 20 ng/ml mIL-18 preincubated with 3 μ g/ml or 12 μ g/ml of the indicated Fc fusion proteins. Luciferase activity, represented as relative light units (RLU), was determined 4 h following stimulation. The experiment was repeated three times, with the data from a typical experiment presented.

precipitation with protein G was specific for the Fc region (Fig. 3). Thus, p13 competes with the IL-18 receptor for cytokine binding.

EV p13 inhibits the activity of IL-18 in vitro

Because p13 inhibits binding of IL-18 to its receptor, one would predict that it also inhibits the biological activity of IL-18. To test this, we preincubated rIL-18 with the indicated purified proteins, then used these mixtures to stimulate COS-7 cells transfected with an NF- κ B-responsive luciferase reporter gene and both IL-18R subunits. Consistent with its inability to bind IL-18 with high avidity, sIL-1Rrp1-Fc displayed no significant inhibition of IL-18 activity in this assay (Fig. 4); however, sIL-1Rrp1-Fc + sAcPL-Fc was an efficient inhibitor, displaying 78% inhibition at an \sim 160-fold molar excess over IL-18. Preincubation of mIL-18 with p13-Fc resulted in a 51% inhibition at an \sim 240-fold molar excess (Fig. 4). p13-FlagpolyHis showed similar inhibition in separate experiments (data not shown).

Specificity of the observed inhibition was demonstrated by the fact that neither sIL-1Rrp1-Fc + sAcPL-Fc nor p13-Fc inhibited IL-1 β stimulated NF- κ B activity (data not shown). The potency of inhibition displayed by sIL-1Rrp1-Fc + sAcPL-Fc relative to p13-Fc is in agreement with the relative avidities we determined by BIAcore measurements (Table I). The lack of inhibition by sIL-1Rrp1-Fc is likely due to the combination of a low avidity of this protein for IL-18, and the fact that the full-length receptors are overexpressed on the COS cell surface in this experiment. We have tested the ability of sIL-1Rrp1-Fc and sIL-1Rrp1-FlagpolyHis to inhibit IL-18-mediated proliferation of the murine T cell line AE7, and do see a modest level of inhibition under these conditions (data not shown).

An in vivo role for p13 in NK cell activation

NK cells are an important component of the innate immune response that contributes to recovery from infection. Because IL-18 is known to induce NK cell cytotoxicity, and our results demonstrate that p13 inhibits the activity of IL-18, it is possible that p13 secretion from EV-infected cells may attenuate the activation of NK cells proximal and/or distal to the site of EV replication. To

test this hypothesis, we constructed an EV deletion mutant in which nt 60–149 of the coding region of the p13 gene (416 nt in length) were deleted and replaced with an *E. coli gpt* selection cassette. The genotype of EV-p13⁻ was confirmed by PCR and DNA sequence analysis. Moreover, Western blot analysis failed to detect p13 protein in the EV-p13⁻-infected cells or culture supernatant (data not shown). This EV deletion mutant was used to investigate the role of p13 in viral pathogenesis using the peritoneal route of infection. This route of inoculation permitted us to measure the kinetics of appearance of NK cytotoxic activity and cytokine production at the site of infection.

EV-p13⁻, EV-WT, or saline was injected into the peritoneum of C57BL/6 mice, and spleens and PECs were collected 1, 2, or 3 days p.i. NK cytotoxic activity was measured using a standard ⁵¹Cr-release assay with YAC-1 tumor cell targets. We did not observe any significant difference between cytotoxic activity associated with splenocytes from EV-p13⁻, EV-WT, or saline-treated animals up to 3 days p.i. (data not shown). In contrast, PECs from EV-p13⁻-infected mice showed progressive and dramatic increases in cytotoxic activity compared with WT virus-infected mice 2 and 3 days p.i. (Fig. 5). The cytotoxic activity was likely due to NK cells in the PECs rather than CTL because the YAC-1 target cells were uninfected and MHC mismatched with the C57BL/6 effectors. To verify that lysis of the targets was attributable to NK cells, PECs collected from mice infected 3 days earlier with EV-p13⁻ were depleted of CD8⁺ cells or CD8⁺ and asialo-GM₁⁺ cells by incubation with Ab and complement. The remaining PECs, without adjustment for reduction of cell numbers due to depletion of CD8⁺ and/or asialo-GM₁⁺ cells, were tested for cytotoxic activity on YAC-1 target cells (Fig. 5D). This assay method ensures that remaining PEC populations would be present at their original concentrations and thus would not bias the anti-target activity. The results indicate that the majority of the cytotoxic activity exhibited by PECs from EV-p13⁻-infected mice is attributable to NK cells. Taken together, these data suggest that NK cell cytotoxic activity at the site of infection was enhanced in mice infected with the EV-p13⁻ relative to EV-WT.

This increase over time in the cytotoxic activity of NK cells from EV-p13⁻-infected mice may be due to increased numbers, or increased activation, of NK cells present in the PEC population. To distinguish these possibilities, NK cells in the peritoneal cavity were enumerated by flow cytofluorometric analysis. In the representative experiment from 3 days p.i., NK1.1⁺ cells comprised 2.3% of the PECs of mice infected with EV-p13⁻, compared with 2.2% and 4.1% of PECs from EV-WT-infected and control mice, respectively (Fig. 6). The total number of cells collected in the peritoneal washes of EV-p13⁻- and EV-WT-infected mice varied by ~53% of the saline control group. A slight increase in the number of CD4⁺ and CD8⁺ cells in the peritoneal cavities of mice infected with EV-p13⁻ was observed, relative to saline-treated animals, 3 days p.i. (Fig. 6). These data suggest that the increased cytotoxic activity observed following infection with p13⁻ mutant virus is due primarily to elevated activation of NK cells in PECs, and not an increased number of NK cells.

As an alternative measure of NK cell activation, cytokine production in splenocytes and PECs was determined by ELISA of culture supernatants. Unfractionated splenocytes from either EV-WT- or EV-p13⁻-infected mice generated similar levels of IFN- γ and IL-10 (data not shown). However, IFN- γ production in PEC cultures from EV-WT-infected mice was 20-fold lower than comparable cultures from saline and EV-p13⁻-infected mice (Table II). This is in agreement with our observations above indicating a difference in NK cell activation in PEC but not splenocytes from EV-p13⁻-infected mice relative to EV-WT infection. Interest-

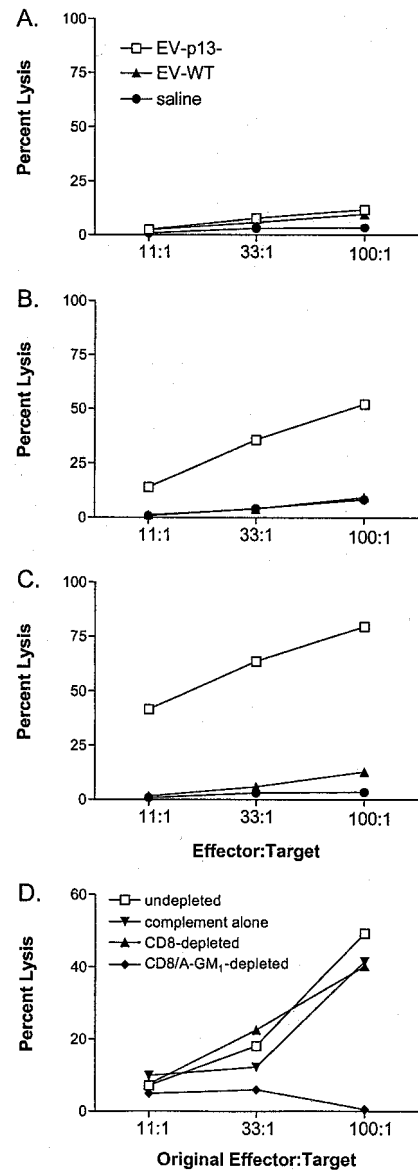


FIGURE 5. Cytolysis of YAC-1 tumor cells by PECs from EV-p13⁻-infected mice. Groups of mice were injected i.p. with EV-WT, EV-p13⁻ or saline. At 1 (A), 2 (B), or 3 (C) days postinjection, PECs were collected and combined at various effector to target ratios with ⁵¹Cr-labeled YAC-1 tumor target cells. Supernatants were collected after a 5-h incubation period, and percent release of radiolabel was determined. Values represent the mean specific release from triplicate cultures. A representative experiment of three performed is shown. D, Ten mice were infected i.p. with 1×10^4 PFU of EV-p13⁻. At 3 days p.i., PECs were collected and pooled. Aliquots of 3×10^6 PECs were incubated with PBS, complement alone, anti-CD8 + complement, or anti-CD8 + complement followed by anti-asialo-GM₁ + complement. To avoid enrichment of undepleted cell types, effector cells were added to ⁵¹Cr-labeled YAC-1 targets without adjustment for cell loss. Samples were analyzed by flow cytometry to confirm depletion. A representative experiment of two performed is shown.

ingly, IL-10 production reproducibly tended to be lower in PECs of mice infected with EV-p13⁻ compared with EV-WT-infected or control mice. These data suggest that the loss of p13 may result in an enhanced type 1 pattern of cytokine production by PECs of EV-infected mice.

The role of p13 in EV replication

Given the observed increase in NK cell activation, we would predict an effect on the pathogenesis of infection in EV-p13⁻-infected

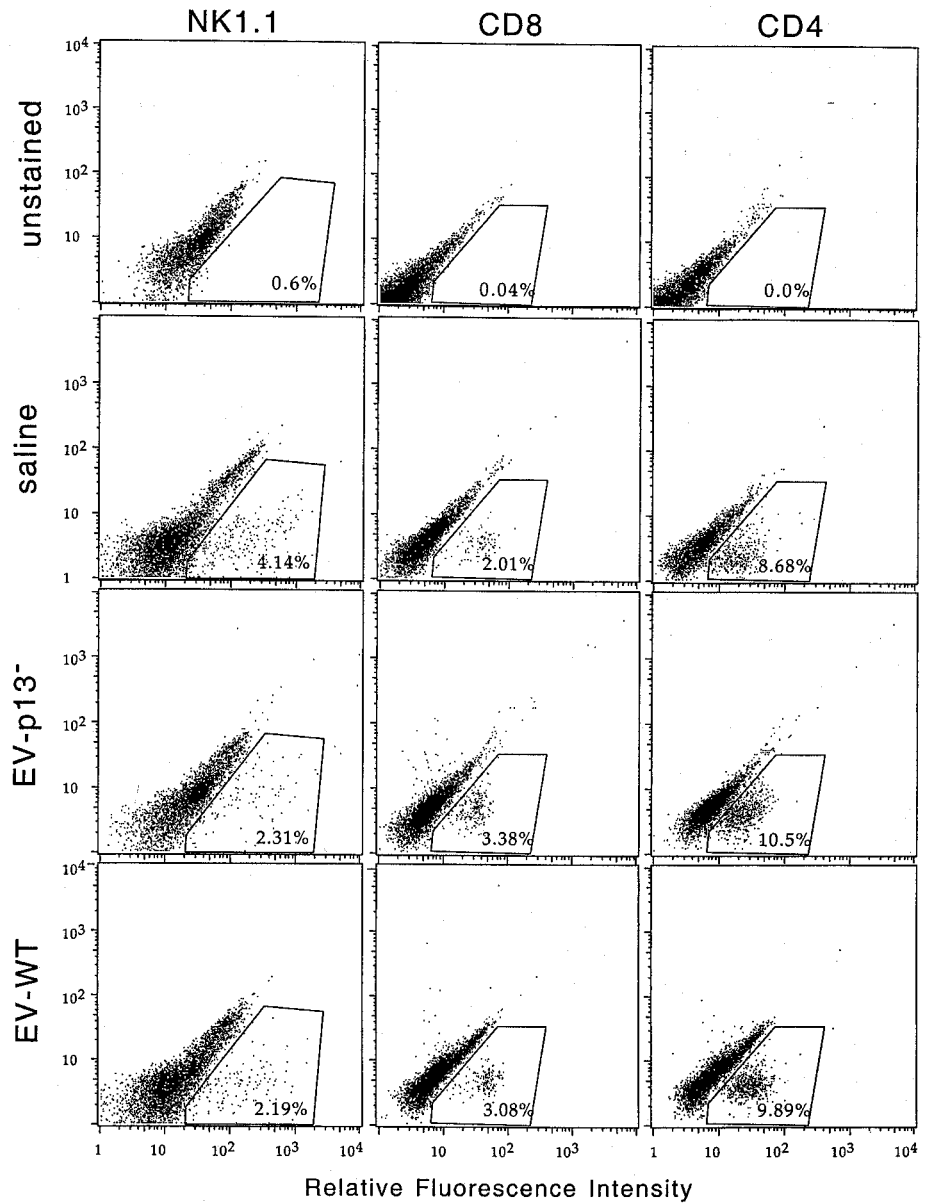


FIGURE 6. Percentage of NK cells in the peritoneal cavities of infected mice is unchanged. Three mice were injected with saline, or 1×10^4 PFU of EV-p13⁻ or EV-WT. Three days p.i., PECs were collected and pooled, stained for cell surface markers NK1.1, CD8, or CD4 using FITC-conjugated mAbs (abscissa), and analyzed by flow cytometry. Gates were set on live cells and on lymphocytes for CD8 and CD4 analyses. Unstained cells are shown at the top of each panel. Isotype control for primary Abs was negative (not shown). A representative experiment of three performed is shown.

mice. To test this hypothesis, groups of mice were injected i.p. with EV-p13⁻ or EV-WT, and virus titers in spleens, livers and peritoneal cavities were determined 3 days p.i. Virus titers in peritoneal washes were similar between the two infections (data not shown). The viral titer in liver and spleen from mice infected with EV-p13⁻ was significantly lower compared with that from EV-

WT-infected animals in one experiment (Table III). When the experiment was repeated with a smaller sample size, we again observed a decrease in viral titer in the liver of mice infected with EV-p13⁻ compared with EV-WT. Splenic titers of EV, however, were similar between EV-p13⁻ and EV-WT-infected mice in the second experiment (Table III). The p13⁻ mutant virus replicates with similar efficiency to WT virus in tissue culture (data not shown), suggesting that at least the difference in infectivity levels in liver may be attributed to the action of host antiviral mechanisms. The correspondence of the p13⁻ deletion with poorer growth rate in liver suggests that binding of IL-18 by p13 may contribute to the capacity of EV to evade host defenses.

Table II. Cytokine production from PECs at 3 days p.i.^a

Treatment Group	Cytokine in Culture Supernatants (ng/ml)	
	IFN- γ	IL-10
EV-p13 ⁻	2.0	24.4 ^b
EV-WT	0.1 ^c	36.3
Saline	3.2	62.7

^a PECs were cultured for 5.5 h in the presence of PMA and Ca²⁺ ionophore. Values represent geometric mean titers from three individual mice/group. SEM was <42% for all groups.

^b Significantly different from saline, $p = 0.017$.

^c Two of three values were below the limit of detection (0.064 ng/ml).

Discussion

We have demonstrated that the secreted p13 protein of EV is able to bind IL-18 and inhibit its activity in vitro. BIAcore measurements suggest that the avidity of IL-18 for the receptor heterodimer ($K_D = 0.2$ nM) is higher than its avidity for p13 ($K_D = 5.0$ nM). This is in agreement with our in vitro inhibition assays, which similarly suggested that sIL-1Rrp1 + sAcPL was a more

Table III. WT and p13⁻ EV titers in various tissues of C57BL/6 mice^a

	Expt. 1 (n = 9)		Expt. 2 (n = 3)	
	Liver	Spleen	Liver	Spleen
EV-WT	$4.0 \times 10^5 \pm 1.4$	$1.2 \times 10^6 \pm 0.2$	$3.8 \times 10^4 \pm 1.5$	$8.4 \times 10^5 \pm 5.7$
EV-p13 ⁻	$0.6 \times 10^5 \pm .14^*$	$0.4 \times 10^6 \pm .09^*$	$0.8 \times 10^4 \pm .07$	$9.8 \times 10^5 \pm 6.6$

^a Groups of C57BL/6 mice were inoculated with 1×10^4 PFU of EV-WT or p13⁻ mutant virus. Values represent mean titers \pm SEM in PFU/g. The same stocks of virus were used in both experiments although the mice were from two separate shipments.

* $p < .05$, compared to EV-WT; two-sided Wilcoxon Rank Sum test.

potent inhibitor of IL-18 than was p13. Since it is likely, however, that IL-18R heterodimers do not exist preformed on the cell surface, the more relevant comparison is apt to be the ability of soluble p13 protein to compete with cell-bound IL-1Rrp1 protein for binding of sIL-18. The avidity of p13 for IL-18 is 5- to 10-fold higher than that of IL-1Rrp1, making it an effective antagonist. In addition, the initial dissociation rate of IL-18 from p13 is quite slow. A slow dissociation rate is advantageous for an inhibitor and, to the extent that heterodimeric cell-surface receptors do form rapidly, might help compensate for the fact that the affinity of p13 is lower than the avidity of the heterodimer. Finally, the robust synthetic capacity of the virus also would likely cause p13 to be present in vast molar excess over the cellular IL-18R.

The maximum RRU shift observed by BIAcore for p13-Fc was consistently higher than that observed for either of the receptor preparations tested. Decreasing the amount of p13-Fc loaded onto the chip decreased the magnitude of the difference. However, we did not observe similar maximal RRU shifts for p13 and the cellular receptors even when equimolar amounts of each protein were loaded (Fig. 2). Furthermore, the binding of IL-18 to p13-Fc did not reach a plateau by 6 min, as did binding to the cellular receptor Fc fusion proteins. These differences observed in the BIAcore binding profiles could be due to a difference in conformation between the smaller p13-Fc (45 kDa) and larger IL-18R-Fc proteins (~85 kDa by SDS-PAGE), resulting in differences in accessibility to cytokine when immobilized on the BIAcore flow cell. Alternatively, it could represent differences in the percentage of active (IL-18 binding) protein in equimolar amounts of total protein, or errors in determination of protein concentration between the samples. Protein concentrations were determined in at least two independent assays and verified by SDS-PAGE and Coomassie stain. Regardless, BIAcore affinity measurements are dependent on the concentration of the soluble analyte (IL-18), but independent of the concentration of the immobilized protein. Each affinity constant was determined for at least two different concentrations of loaded Fc fusion protein, and in all cases the results were consistent.

It is well established that recruitment of AcP to the active IL-1/IL-1R complex increases its stability. In stably transfected CHO cells, an ~4-fold increase in affinity has been reported in the presence of AcP (38). In EL4 cells, the K_D of IL-1 α has been reported to be the same for cells expressing or lacking AcP, yet the stability of binding was increased in the presence of AcP, suggesting that AcP most likely alters the off rate of IL-1 from the receptor complex (39). A similar alteration in the binding of IL-18 would be expected in the presence of AcPL, yet the results reported above offer the first direct examination of this issue. Our in vitro assays, such as immunoprecipitation and BIAcore binding, suggest an increased avidity of IL-18 for the receptor heterodimer (sIL-1Rrp1-Fc/sAcPL-Fc) as compared with its avidity toward sIL-1Rrp1-Fc alone. It should be noted, however, that due to inadequacies of current Abs, we have not formally demonstrated the presence of receptor heterodimers in our sIL-1Rrp1-Fc/sAcPL-Fc cotrans-

fected cell supernatants. We have assumed that the differences we observe in this protein preparation as compared with IL-1Rrp1-Fc protein are due to the presence of heterodimeric soluble receptor molecules. An independent approach to verify the altered avidity of the receptor heterodimer is needed. We have attempted these experiments in standard cell-surface binding experiments, and have had difficulties with background IL-18 binding which makes quantitative results inconclusive. In qualitative assays, however, we have observed a higher level of iodinated IL-18 binding to cells overexpressing both receptor subunits relative to cells overexpressing IL-1Rrp1 alone (data not shown).

The demonstration that EV p13 binds IL-18 with high avidity in vitro suggested that it has the capacity to sequester IL-18 in vivo, affecting the innate immune response to EV infection. To test this possibility, we constructed an EV mutant in which the p13 gene was deleted and then monitored NK cell activation and cytokine production in infected C57BL/6 mice. We wished to examine the activation of NK cells both proximal and distal to the initial site of infection. EV infects mice in the wild through minor skin abrasions, yet it is technically difficult to quantitate, and to measure the activation state of, NK cells entering epidermal/dermal lesions. Therefore, we chose to infect mice by the i.p. route and measure NK cell numbers and activation state in spleen and peritoneal cavity. The most dramatic differences between WT-EV and EV-p13⁻ infections were observed in NK cells proximal to the site of infection (from the peritoneal cavity). First, PECs from p13⁻ virus-infected mice showed a progressive increase in NK-associated cytotoxic activity against YAC-1 targets as compared with samples from EV-WT or saline controls. The elevated NK cell cytotoxicity was not due to enhanced trafficking of NK1.1⁺ cells into the peritoneal cavity, as mice injected with EV-WT, EV-p13⁻, or saline had similar numbers of NK1.1⁺ PECs over a 3-day period. Rather, the elevated cytotoxicity is likely due to an increased frequency of activated NK cells in PECs of EV-p13⁻-infected mice. This is consistent with the lack of an IL-18BP in the p13⁻ virus, because IL-18 is known to activate NK cells, at least in part, through stimulation of Fas ligand-mediated cytotoxicity (40, 41). Second, higher levels of IFN- γ were observed in PECs of mice infected with EV-p13⁻ compared with those infected with EV-WT. This is consistent with the observed increase in NK cytotoxic activity in PECs of EV-p13⁻-infected mice, and with the fact that IL-18 is a potent inducer of IFN- γ . The enhanced IFN- γ production was observed proximal to the initial site of infection but not distally in the spleen. While this correlated with our data indicating a lack of splenic NK cytotoxic activation, the reasons for differential NK cell activation between PECs and splenocytes remain unresolved.

Titer of virus in the peritoneal cavity, to which abdominal organs as well as resident PECs contribute, was not significantly affected by increased NK cytotoxic activity or IFN- γ secretion by PECs in p13⁻ virus-infected mice. However, liver titers were significantly influenced by loss of p13. A number of factors could affect the phenotype of p13⁻ mutant in various cells and tissues. It

has been shown that IL-18-dependent responses can differ according to the tissue source of the treated cell. For example, studies have shown that liver lymphocytes respond to IL-18 by production of IFN- γ , and that this production can occur independently of IL-12 (42). In contrast, splenic T cells from C57BL/6 mice apparently do not produce IFN- γ in response to IL-18, alone or in combination with IL-12 (43), and indeed, we did not find elevated IFN- γ production or NK activity in the spleen of EV-p13⁻-infected mice. Also, in a recent study the effectiveness of IFN- γ in controlling EV replication was shown to vary among tested tissues (44). And finally, EV-infected splenocytes, PECs, or liver cells may differ in effectiveness as targets of NK-mediated cytotoxicity. These observations may help to explain the differential IFN- γ production, NK activation, and viral titer we detected in cells from the liver, spleen and peritoneal cavity of infected mice. Further work will be required to determine whether NK activity is elevated in the liver of EV-p13⁻-infected mice, and the suitability of cell types in the various organs as NK targets.

NK cells, and their capacity to secrete IFN- γ , are critical in the early defense against infection by viral pathogens, and are targets of poxvirus host response modifier genes. EV-infected cells secrete a binding protein with high affinity for IFN- γ ($K_D \sim 1$ nM) (45, 46). Also, EV-infected cells synthesize a double-stranded RNA binding protein (E3L) which blocks IFN- γ action by inhibiting dsRNA-activated protein kinase and 2'-5' oligonucleotide adenylate synthase (47). IL-18 is an important inducer of IFN- γ production and cytotoxicity, and it appears that EV can inhibit IL-18 action through multiple mechanisms. It has been shown that the orthopoxvirus *crm* A gene, which is expressed by EV, blocks the action of IL-1 β -converting enzyme, a protease that converts both the IL-1 β and IL-18 precursors into mature forms (48). Because *crm* A is a cytoplasmic protein, it can only affect IL-18 maturation in the infected cell, conceivably allowing IL-18 secretion by uninfected neighboring cells triggered by inflammatory mediators. The discovery that EV p13 encodes a secreted protein that binds and inactivates IL-18 suggests that EV may also have a mechanism to block IL-18 action at a distance from the infected cell. Together *crm* A and p13 would provide the virus with a means to inhibit IL-18-mediated NK cell activation proximal to a focus of infection. It is probable that the effectiveness of IL-18 inhibition will vary from tissue to tissue, but likely would be greatest in the skin, the primary site of infection and transmission.

Although IL-18 has been shown to affect differentiation and expansion of Th1 cells, we believe the importance of poxvirus IL-18BP homologues to the virus life cycle will reside in the attenuation of NK, or perhaps memory T cell, effector function. This hypothesis is based on several observations. *Molluscum contagiosum* virus encodes at least three IL-18BP homologues (49), yet replicates only in keratinocytes of the human epidermis, at a distance from any T cell-rich lymphoid organ. The epidermal keratinocytes are major producers of IL-18 (50), and mouse skin is a source of potentially IL-18-responsive NK, NK-like, or memory T cells (51, 52). Finally, NK and memory T cells have been shown to be important in controlling poxvirus infections (21, 53).

Acknowledgments

We thank Mike Comeau, Jeff Bradshaw, and Melissa Petersen for p13-Fc and p13-FlagpolyHis plasmid constructions and protein purification; Dirk Anderson for sequence communication; Lynn Dustin for advice on flow cytometric analysis; Li Zhu and Bruce Kelly for technical assistance; Anyang Feng for statistical analysis; and Lisa Sedger, Linda Park, and David Cosman for critical review of the manuscript.

References

- Okamura, H., H. Tsutsui, S. Kashiwamura, T. Yoshimoto, and K. Nakanishi. 1998. Interleukin-18: a novel cytokine that augments both innate and acquired immunity. *Adv. Immunol.* 70:281.
- Gillespie, M. T., and N. J. Horwood. 1998. Interleukin-18: perspectives on the newest interleukin. *Cytokine Growth Factor Rev.* 9:109.
- Okamura, H., H. H. Tsutsui, T. Komatsu, M. Yutsudo, A. Hakura, T. Tanimoto, K. Torigoe, T. Okura, Y. Nukada, K. Hattori, et al. 1995. Cloning of a new cytokine that induces interferon γ production by T-cells. *Nature* 378:88.
- Takeda, K., H. Tsutsui, T. Yoshimoto, O. Adachi, N. Yoshida, T. Kishimoto, H. Okamura, K. Nakanishi, and S. Akira. 1998. Defective NK cell activity and Th1 response in IL-18-deficient mice. *Immunity* 8:383.
- Kohno, K., J. Kataoka, T. Ohtsuki, Y. Suemoto, I. Okamoto, M. Usui, M. Ikeda, and M. Kurimoto. 1997. IGIF is a costimulatory factor on the activation of Th1 but not Th2 cells and exerts its effect independently of IL-12. *J. Immunol.* 158:1541.
- Micallef, M. J., T. Ohtsuki, K. Kohno, F. Tanabe, S. Ushio, M. Namba, T. Tanimoto, K. Torigoe, M. Fujii, M. Ikeda, S. Fukuda, and M. Kurimoto. 1996. Interferon- γ -inducing factor enhances T helper 1 cytokine production by stimulated human T cells: synergism with interleukin-12 for interferon- γ production. *Eur. J. Immunol.* 26:1647.
- Hunter, C. A., J. Timans, P. Pisacane, S. Menon, G. Cai, W. Walker, M. Aste-Amezaga, R. Chizzonite, J. F. Bazan, and R. A. Kastelein. 1997. Comparison of the effects of interleukin-1 α , interleukin-1 β and interferon- γ -inducing factor on the production of interferon- γ by natural killer. *Eur. J. Immunol.* 27:2787.
- Tsutsui, H., K. Matsui, N. Kawada, Y. Hyodo, N. Hayashi, H. Okamura, K. Higashino, and K. Nakanishi. 1997. IL-18 accounts for both TNF- α - and Fas ligand-mediated hepatotoxic pathways in endotoxin-induced liver injury in mice. *J. Immunol.* 159:3961.
- Hyodo, Y., K. Matsui, N. Hayashi, H. Tsutsui, S.-i. Kashiwamura, H. Yamauchi, K. Hiroishi, K. Takeda, Y.-i. Tagawa, Y. Iwakura, et al. 1999. IL-18 up-regulates perforin-mediated NK activity without increasing perforin messenger RNA expression by binding to constitutively expressed IL-18 receptor. *J. Immunol.* 162:1662.
- Dao, T., W. Z. Mehal, and I. N. Crispe. 1998. IL-18 augments perforin-dependent cytotoxicity of liver NK-T cells. *J. Immunol.* 161:2217.
- Bazan, J. F., J. C. Timans, and R. A. Kastelein. 1996. A newly defined interleukin-1? *Nature* 379:591.
- Gu, Y., K. Kuida, H. Tsutsui, G. Ku, K. Hsiao, M. A. Fleming, N. Hayashi, K. Higashino, H. Okamura, K. Nakanishi, et al. 1997. Activation of IFN γ inducing factor mediated by ICE. *Science* 275:206.
- Ghayur, T., S. Banerjee, M. Hugunin, D. Butler, L. Herzog, A. Carter, L. Quintal, L. Sekut, R. Talanian, M. Paskind, et al. 1997. Caspase-1 processes IFN γ inducing factor and regulates LPS induced IFN γ induction. *Nature* 386:619.
- Torigoe, K., S. Ushio, T. Okura, S. Kobayashi, M. Taniai, T. Kunikata, T. Murakami, O. Sanou, H. Kojima, M. Fujii, et al. 1997. Purification and characterization of the interleukin-18 receptor. *J. Biol. Chem.* 272:25737.
- Thomassen, E., T. A. Bird, B. R. Renshaw, M. K. Kennedy, and J. E. Sims. 1998. Binding of interleukin-18 to the interleukin-1 receptor homologous receptor IL-1Rrp1 leads to activation of signaling pathways similar to those used by interleukin-1. *J. Interferon Cytokine Res.* 18:1077.
- Born, T. L., E. Thomassen, T. A. Bird, and J. E. Sims. 1998. Cloning of a novel receptor subunit, AcPL, required for interleukin-18 signaling. *J. Biol. Chem.* 273:29445.
- Ahn, H.J., S. Maruo, M. Tomura, J. Mu, T. Hamaoka, K. Nakanishi, S. Clark, M. Kurimoto, H. Okamura, and H. Fujiwara. 1997. A mechanism underlying synergy between IL-12 and IFN- γ -inducing factor in enhanced production of IFN- γ . *J. Immunol.* 159:2125.
- Yoshimoto, T., K. Takeda, T. Tanaka, K. Ohkusu, S. Kashiwamura, H. Okamura, S. Akira, and K. Nakanishi. 1998. IL-12 up-regulates IL-18 receptor expression on T cells, Th1 cells, and B cells: synergism with IL-18 for IFN- γ production. *J. Immunol.* 161:3400.
- Novick, D., S. H. Kim, G. Fantuzzi, L. L. Reznikov, C. A. Dinarello, and M. Rubinstein. 1999. Interleukin-18 binding protein: a novel modulator of the Th1 cytokine response. *Immunity* 10:127.
- Senkevich, T. G., E. V. Koonin, and R. M. Buller. 1994. A poxvirus protein with a RING zinc finger motif is of crucial importance for virulence. *Virology* 198:118.
- Buller, R. M., and G. J. Palumbo. 1991. Poxvirus pathogenesis. *Microbiol. Rev.* 55:80.
- Spriggs, M. K. 1996. One step ahead of the game: viral immunomodulatory molecules. *Annu. Rev. Immunol.* 14:101.
- Smith, C. A., T. Davis, J. M. Wignall, W. S. Din, T. Farrah, C. Upton, G. McFadden, and R. G. Goodwin. 1991. T2 open reading frame from the Shope fibroma virus encodes a soluble form of the TNF receptor. *Biochem. Biophys. Res. Commun.* 176:335.
- Upton, C., J. L. Macen, M. Schreiber, and G. McFadden. 1991. Myxoma virus expresses a secreted protein with homology to the tumor necrosis factor receptor gene family that contributes to viral virulence. *Virology* 184:370.
- Smith, C. A., T. D. Smith, P. J. Smolak, D. Friend, H. Hagen, M. Gerhart, L. Park, D. J. Pickup, D. Torrance, K. Mohler, et al. 1997. Poxvirus genomes encode a secreted, soluble protein that preferentially inhibits β chemokine activity yet lacks sequence homology to known chemokine receptors. *Virology* 236:316.

26. Graham, K. A., A. S. Lalani, J. L. Macen, T. L. Ness, M. Barry, L. Y. Liu, A. Lucas, I. Clark-Lewis, R. W. Moyer, and G. McFadden. 1997. The T1/35 kDa family of poxvirus-secreted proteins bind chemokines and modulate leukocyte influx into virus-infected tissues. *Virology* 229:12.
27. Lalani, A. S., K. Graham, K. Mossman, K. Rajarathnam, I. Clark-Lewis, D. Kelvin, and G. McFadden. 1997. The purified myxoma virus gamma interferon receptor homolog M-T7 interacts with the heparin-binding domains of chemokines. *J. Virol.* 71:4356.
28. Alcami, A., J. A. Symons, P. D. Collins, T. J. Williams, and G. L. Smith. 1998. Blockade of chemokine activity by a soluble chemokine binding protein from vaccinia virus. *J. Immunol.* 160:624.
29. Giri, J. G., M. Ahdieh, J. Eisenman, K. Shanebeck, K. Grabstein, S. Kumaki, A. Namen, L. S. Park, D. Cosman, and D. Anderson. 1994. Utilization of the β and γ chains of the IL-2 receptor by the novel cytokine IL-15. *EMBO J.* 13:2822.
30. Baum, P. R., R. B. Gayle, F. Ramsdell, S. Srinivasan, R. A. Sorensen, M. L. Watson, M. F. Seldin, E. Baker, G. R. Sutherland, K. N. Clifford, et al. 1994. Molecular characterization of murine and human OX40/OX40 ligand systems: identification of a human OX40 ligand as the HTLV-1-regulated protein gp34. *EMBO J.* 13:3992.
31. Mitchell, T., and B. Sudegen. 1995. Stimulation of NF- κ B-mediated transcription by mutant derivatives of the latent membrane protein of Epstein-Barr virus. *J. Virol.* 69:2968.
32. Kozlosky, C. J., E. Maraskovsky, J. T. McGrew, T. VandenBos, M. Teepe, S. D. Lyman, S. Srinivasan, F.A. Fletcher, R.B. Gayle, D. P. Cerretti, and M. P. Beckmann. 1995. Ligands for the receptor tyrosine kinases hek and elk: isolation of cDNAs encoding a family of proteins. *Oncogene* 10:299.
33. Cosman, D., D. P. Cerretti, A. Larsen, L. Park, C. March, S. Dower, S. Gillis, and D. Urdal. 1984. Cloning, sequence and expression of human interleukin-2 receptor. *Nature* 312:768.
34. Johnsson, B., S. Lofas, and G. Lindquist. 1991. Immobilization of proteins to a carboxymethyl-dextran-modified gold surface for biospecific interaction analysis in surface plasmon resonance sensors. *Anal. Biochem.* 198:268.
35. Chen, W., R. Drillien, D. Spehner, and R. M. Buller. 1992. Restricted replication of ectromelia virus in cell culture correlates with mutations in virus-encoded host range gene. *Virology* 187:433.
36. Karupiah, G., R. M. Buller, N. Van Rooijen, C. J. Duarte, and J. Chen. 1996. Different roles for CD4⁺ and CD8⁺ T lymphocytes and macrophage subsets in the control of a generalized virus infection. *J. Virol.* 70:8301.
37. Karupiah, G., B. E. Coupar, M. E. Andrew, D. B. Boyle, S. M. Phillips, A. Mullbacher, R. V. Blanden, and I. A. Ramshaw. 1990. Elevated natural killer cell responses in mice infected with recombinant vaccinia virus encoding murine IL-2. *J. Immunol.* 144:290.
38. Greenfeder, S. A., P. Nunes, L. Kwee, M. Labow, R. A. Chizzonite, and G. Ju. 1995. Molecular cloning and characterization of a second subunit of the interleukin-1 receptor complex. *J. Biol. Chem.* 270:13757.
39. Wesche, H., K. Resch, and M. U. Martin. 1998. Effects of IL-1 receptor accessory protein on IL-1 binding. *FEBS Lett.* 429:303.
40. Tsutsui, H., K. Nakanishi, K. Matsui, K. Higashino, H. Okamura, Y. Miyazawa, and K. Kaneda. 1996. IFN- γ -inducing factor up-regulates Fas ligand-mediated cytotoxic activity of murine natural killer cell clones. *J. Immunol.* 157:3967.
41. Dao, T., K. Ohashi, T. Kayano, M. Kurimoto, and H. Okamura. 1996. Interferon- γ -inducing factor, a novel cytokine, enhances Fas ligand-mediated cytotoxicity of murine T helper 1 cells. *Cell. Immunol.* 173:230.
42. Matsui, K., T. Yoshimoto, H. Tsutsui, Y. Hyodo, N. Hayashi, K. Hiroishi, N. Kawada, H. Okamura, K. Nakanishi, and K. Higashino. 1997. Propionibacterium acnes treatment diminishes CD4⁺ NK1.1⁺ T cells but induces type I T cells in the liver by induction of IL-12 and IL-18 production from Kupffer cells. *J. Immunol.* 159:97.
43. Robinson, D., K. Shibuya, A. Mui, F. Zonin, E. Murphy, T. Sana, S. B. Hartley, S. Menon, R. Kastelein, F. Bazan, and A. O'Garra. 1997. IGIF does not drive Th1 development but synergizes with IL-12 for interferon- γ production and activates IRAK and NF- κ B. *Immunity* 7:571.
44. Karupiah, G., T. N. Fredrickson, K. L. Holmes, L. H. Khairallah, and R. M. Buller. 1993. Importance of interferons in recovery from mousepox. *J. Virol.* 67:4214.
45. Upton, C., K. Mossman, and G. McFadden. 1992. Encoding of a homolog of the IFN- γ receptor by myxoma virus. *Science* 258:1369.
46. Mossman, K., C. Upton, R. M. Buller, and G. McFadden. 1995. Species specificity of ectromelia virus and vaccinia virus interferon- γ binding proteins. *Virology* 208:762.
47. Chang, H. W., J. C. Watson, and B. L. Jacobs. 1992. The E3L gene of vaccinia virus encodes an inhibitor of the interferon-induced, double-stranded RNA-dependent protein kinase. *Proc. Natl. Acad. Sci. USA* 89:4825.
48. Turner, S., B. Kenshole, and J. Ruby. 1999. Viral modulation of the host response via crmA/SPI-2 expression. *Immunol. Cell Biol.* 77:236.
49. Xiang, Y., and B. Moss. 1999. Identification of human and mouse homologs of the MC51L-53L-54L family of secreted glycoproteins encoded by the *Molluscum contagiosum* poxvirus. *Virology* 257:297.
50. Stoll, S., G. Muller, M. Kurimoto, J. Saloga, T. Tanimoto, H. Yamauchi, H. Okamura, J. Knop, and A. H. Enk. 1997. Production of IL-18 (IFN- γ -inducing factor) messenger RNA and functional protein by murine keratinocytes. *J. Immunol.* 159:298.
51. Romani, N., G. Stingl, E. Tschachler, M. D. Witmer, R. M. Steinman, E. M. Shevach, and G. Schuler. 1985. The Thy-1-bearing cell of murine epidermis: a distinctive leukocyte perhaps related to natural killer cells. *J. Exp. Med.* 161:1368.
52. Bos, J. D., and M. L. Kapsenberg. 1993. The skin immune system: progress in cutaneous biology. *Immunol. Today* 14:75.
53. Ikeda, S., T. Tominaga, and C. Nishimura. 1991. Thy1⁺ asialo GM1⁺ dendritic epidermal cells in skin defense mechanisms of vaccinia virus-infected mice. *Arch. Virol.* 117:207.